HHS Public Access

Author manuscript

Nat Neurosci. Author manuscript; available in PMC 2017 November 15.

Published in final edited form as:

Nat Neurosci. 2017 July ; 20(7): 978–986. doi:10.1038/nn.4563.

Identification of a motor to auditory pathway important for vocal learning

Todd F. Roberts[1,*,†], **Erin Hisey**[2,†], **Masashi Tanaka**[2], **Matthew Kearney**[2], **Gaurav Chattree**[1], **Cindy F. Yang**[3,4], **Nirao M. Shah**[4], and **Richard Mooney**[2,*]

[1]Department of Neuroscience, University of Texas Southwestern Medical Center, Dallas, TX 75390, USA

[2]Department of Neurobiology, Duke University Medical Center, Durham, NC 27710, USA

[3]Program in Neuroscience, University of California San Francisco, San Francisco, CA 94158, USA

[4]Department of Psychiatry, Stanford University, Stanford, CA 94305, USA

Summary

Learning to vocalize depends on the ability to adaptively modify the temporal and spectral features of vocal elements. Neurons that convey motor-related signals to the auditory system are theorized to facilitate vocal learning, but the identity and function of such neurons remain unknown. Here we identify a previously unknown neuron type in the songbird brain that transmits vocal motor signals to the auditory cortex. Genetically ablating these neurons in juveniles disrupted their ability to imitate features of an adult tutor's song. Ablating these neurons in adults had little effect on previously learned songs, but interfered with their ability to adaptively modify the duration of vocal elements and largely prevented the degradation of song's temporal features normally caused by deafening. These findings identify a motor to auditory circuit essential to vocal imitation and to the adaptive modification of vocal timing.

Learning complex motor sequences, such as those required for speech or musical expression depends on rapid and precise sensorimotor interactions. Auditory to motor interactions are evident in the important role that auditory experience plays in speech and musical learning. Motor to sensory interactions are manifest in the motor-related signals that are readily detected in many sensory brain regions, including the auditory system [1–4]. Such motor to

*Correspondence to: Todd Roberts (todd.roberts@utsouthwestern.edu) and Richard Mooney (mooney@neuro.duke.edu).
†These authors contributed equally to this work.
Correspondence and requests for materials should be addressed to T.F.R. (todd.roberts@utsouthwestern.edu) and R.M. (mooney@neuro.duke.edu).

Author contributions: T.F.R., E.H. and R.M. conceived and designed all experiments. T.F.R. did the anatomical tracing experiments, juvenile genetic lesion experiments, and designed and oversaw the conditional auditory feedback experiments. E.H. did the anatomical tracing experiments, adult genetic lesioning experiments and adult deafening experiments. M.T., M.K., and G.C. did the slice physiology, calcium imaging and conditional auditory feedback experiments, respectively. C.F.Y. and N.M.S. provided virus used for cell ablation experiments. T.F.R. and R.M. wrote the manuscript. All authors read and commented on the manuscript.

The authors declare no competing financial interests.

sensory (i.e., forward) signals are thought to facilitate skill learning, including speech and musical learning, through various processes including cancellation of motor-related sensory feedback and predictive computations that give rise to learning-related error signals [5–13]. The neurons and circuits that convey forward signals important to vocal learning remain unknown.

The zebra finch is an oscine songbird that exhibits many striking parallels to humans in its capacity for vocal learning [14]. Zebra finches copy the temporal and spectral features of a tutor's song during a juvenile sensitive period, use auditory feedback to maintain stable adult song, and can adaptively modify the timing and frequency of individual song elements in response to aversive auditory cues [15–18]. The zebra finch's brain contains a specialized network for singing, song learning, and feedback-dependent song maintenance, facilitating the establishment of causal links between neurons, circuits, and learned vocal behavior [19–21]. Consequently, the zebra finch brain affords a promising site to search for neurons and circuits that enable forward interactions important to vocal learning.

One hint of forward interactions are the vocal motor-related signals that have been detected in the zebra finch auditory cortex, reminiscent of the vocalization-related corollary discharge signals observed in the human auditory cortex [22,23]. In the zebra finch, one potential source of motor to auditory signals is the telencephalic nucleus HVC, which generates premotor activity important to song timing [20,24,25]. Two projection neuron (PN) types have been identified in HVC [26], including one (HVC_{RA}) that innervates the song motor nucleus RA and another (HVC_X) that innervates a basal ganglia region (Area X) important to juvenile song learning and adult vocal plasticity [16,27,28]. HVC also makes sparse projections to a small cluster of neurons (Avalanche, or Av) embedded in the caudal mesopallium (CM), an analogue of the mammalian secondary auditory cortex [29]. Although this projection could convey forward signals, the neurons that give rise to this projection have not been identified and their function in song learning remains unknown.

Here we identify that the PNs that link HVC to Av are distinct from HVC_{RA} and HVC_X cells. These HVC_{Av} cells transmit vocal motor-related information to the auditory system, play an essential role in juvenile song copying, and are necessary to the adaptive modification of temporal but not spectral features of the adult's song. These findings provide the first neuronal and circuit candidates for a forward mechanism important to vocal learning.

RESULTS

A distinct neuron type projects from HVC to the auditory system

To identify the HVC neurons project to Av, we injected different color fluorescent retrograde tracers into Av, RA, and Area X (Fig. 1a–b, n = 7 adult birds (> 100 days post hatch (d)), n = 3 juvenile birds (60 d), Av (dextran, Alexa Fluor 594), RA (dextran, Alexa Fluor 488), and Area X (fast blue); all three regions were accurately targeted in 70% of cases, 9/14 hemispheres in adult birds, 5/6 hemispheres in juvenile birds). All injections that successfully targeted Av, as determined by retrograde label in two of its other known afferents (the thalamic nucleus uvaeformis (Uva) and NIf), also retrogradely labeled a

sparsely distributed population of HVC neurons. In contrast, injections targeting regions immediately dorsal or ventral to Av did not label HVC neurons in either juvenile or adult animals (n = 6 hemispheres from 6 animals). Notably, HVC neurons that were labeled by tracer injections in Av were not co-labeled by tracers injected either in Area X or RA (Fig. 1b; n = 14 hemispheres from 10 animals). These findings suggest that the axonal projection from HVC to Av arises from a previously unrecognized PN type (i.e., the HVC_{Av} neuron) and not from the axon collaterals of HVC_{RA} or HVC_{X} neurons.

To better characterize HVC_{Av} neuronal morphology, we injected fluorescent retrograde tracers or a retrogradely transported GFP-expressing virus (AAV2/9-GFP) into Av in a separate cohort of male zebra finches (n = 20 birds). Confocal analysis in fixed tissue revealed that HVC_{Av} neurons possess stellate dendrites with sparsely distributed spines, oblong cell bodies, and an axon that exits along HVC's rostral – ventral border (Fig. 1c, dendritic radial extent: 140.21 ± 4.98 μm, 29 cells, 3 birds; 0.16 spines/μm, n = 460 spines across 2929 μm of dendrite, 10 cells, 2 birds; soma diameter: 18.61 ± 0.87 μm, 29 cells, 3 birds). Although the extent of dendritic labeling using retrograde expression of GFP could be variable and should be interpreted cautiously, the mean radius of HVC_{Av} cell dendrites (140.21 ± 4.98 μm) was intermediate between reported values for HVC_{X} and HVC_{RA} cells (168 ± 4 μm and 123 ± 0.9 μm, respectively; [30]). Analysis of GFP-expressing HVC_{Av} neurons revealed that the long axis of their cell bodies overlapped with the mean diameters of HVC_{X} and HVC_{RA} cell bodies, whereas the mean somatic area of HVC_{Av} cell bodies overlapped with HVC_{RA} but not HVC_{X} cells, consistent an oblong shape (Supplementary Figure 1; GFP-expressing HVC_{X} and HVC_{RA} cells from Tschida and Mooney, 2012 were reanalyzed here).

We observed that HVC_{Av} neurons constitute only a small percentage of HVC PNs (130 ± 69.8 neurons/hemisphere, 26 hemispheres, 17 birds; ≤ 1%, estimates of HVC neuron numbers vary between 50,000 and 100,000 per hemisphere [26,31]), and appeared to be evenly distributed throughout HVC, resulting in a tiled appearance (Fig. 1b). In contrast to HVC_{X} and HVC_{RA} axons, HVC_{Av} axons did not extend local collaterals within HVC. Therefore, HVC_{Av} neurons may function primarily to transmit signals to Avalanche.

Neurons with different postsynaptic targets often exhibit physiological differences that correspond to different functional roles [30,32–34]. We used visually targeted whole-cell current clamp recordings in brain slices to record from HVC_{Av}, HVC_{X} or HVC_{RA} neurons retrogradely labeled with fluorescent tracers. We found that HVC_{Av} neurons exhibited no spontaneous action potential activity but fired at high rates with little spike rate accommodation when depolarized (Fig. 1d). The intrinsic properties of HVC_{Av} neurons differed from those of HVC_{X} or HVC_{RA} neurons with respect to spike adaptation, spike gain, input resistance, the amplitude of hyperpolarization-activated cation currents (I_h), and the coefficient of variation in DC-evoked interspike intervals (Fig. 1d–i). Therefore, HVC_{Av} neurons can be distinguished from the other two HVC PN types by their axonal projections to the auditory system and by their intrinsic electrical properties.

HVC_{AV} neurons transmit song motor-related signals

Electrical and optical recordings in freely singing birds indicate that HVC_X and HVC_{RA} neurons transmit motor-related activity [24,35–38]. To begin to characterize the functional properties of HVC_{Av} neurons, we monitored their activity in freely singing adult zebra finches using *in vivo* calcium imaging methods. We expressed genetically encoded calcium indicators in HVC_{Av} neurons by injecting a retrogradely transported virus (AAV2/9-CAG-GCaMP6s; n = 3 birds) into Av or, in another bird, by injecting a Cre-dependent virus (AAV2/1-FLEX-CAG-GCaMP6s) into HVC and a retrogradely transported Cre-recombinase containing virus (AAV2/9-CMV-Cre) in Av. A 1 mm diameter GRIN lens was implanted over HVC and calcium transients were detected using a miniaturized head-mounted fluorescent microscope (Fig. 2a, b; n = 4 adult birds). In all four birds, bulk signals were collected across the entire imaging field. In one of these four birds putative cell bodies were discernible in the raw images (Supplementary Movie 1), which we subsequently subjected to automated region of interest (ROI) analysis using a modified constrained non-negative factorization (CNMF) algorithm adapted for single photon data [39].

Singing was accompanied by significant increases in bulk calcium signals in HVC, whereas little or no changes were detected in HVC when birds were not vocalizing (49/49 songs in 4 birds showed > 2 S.D. increase in fluorescence relative to a pre-song baseline, Fig. 2c; Supplementary Fig. 2). Calcium signals increased prior to song onset, consistent with a premotor signal (135.74 ± 54.93 milliseconds before song onset for 49 songs from 4 birds where signal onsets were defined as dF/F increases 2 S.D. above baseline). In the one bird in which calcium transients in putative cell bodies could be detected, different ROIs displayed different singing-related activity patterns, whereas activity patterns of individual ROIs exhibited consistent temporal profiles from one rendition of the song motif to the next (Fig. 2c–e; Supplementary Fig. 2). Although all ROIs showed increased activity during singing, increases in some ROIs could precede song onset, whereas increases in others occurred during the motif (Fig. 2e; Supplementary Figure 2). The temporal profiles of all ROIs isolated using CNMF were prolonged and in many cases persisted following song offset (Fig. 2e). The prolonged transients measured in individual ROIs are likely to be a characteristic of the indicator rather than a special property of HVC_{AV} cells, because the distribution of decay time constants of calcium transients measured in putative HVC_{Av} neurons was indistinguishable from the distribution of decay time constants measured from a mixed population of GCaMP6s-expressing HVC neurons imaged during singing in another bird (Supplementary Fig. 2). Finally, the summed activity of putative HVC_{Av} cell bodies in the fourth bird resembled the bulk signals collected in the other three birds (Supplementary Fig. 2), suggesting that the bulk signals largely reflected somatic activity of retrogradely labeled HVC_{Av} neurons.

The increased activity prior to song onset is consistent with the idea that HVC_{Av} neurons convey a motor-related signal. To further test this idea, we imaged HVC_{Av} neuron activity in a subset of birds before and after deafening (n = 2 birds from which bulk signals were recorded, one in which putative cell bodies were also detected; deafening was achieved by bilateral removal of the cochlea). We found that singing-related activity of HVC_{Av} neurons persisted after deafening (Figure 2c, f; Supplementary Movie 2; 29/30 songs in 2 birds

showed > 2 S.D. increase in fluorescence over a pre-song baseline). Furthermore, the singing-related activity patterns observed after deafening were qualitatively similar to those measured previously with intact hearing, including transients that occurred prior to song onset and that were reproducible across motifs (Fig. 2f; Supplementary Fig. 2; bulk signal activity increased 112.11 ± 61.72 milliseconds before song onset, n = 30 songs, 2 birds). These findings support the idea that singing-related activity in HVC_{Av} neurons is motor-related.

Neurons important to song timing synapse on HVC_{Av} neurons

Various findings indicate that HVC_{RA} neurons are a source of premotor signals that contribute to song timing and that HVC_X neurons convey song motor-related information to the basal ganglia [24,35–38,40]. As HVC_{RA} and HVC_X axon collaterals form excitatory synapses with other HVC neurons [41], either or both PNs could transmit motor-related signals to HVC_{Av} neurons. To clarify which of these PN types provide input to HVC_{Av} neurons, we made visually targeted whole-cell recordings from retrogradely labeled HVC_{Av} neurons in brain slices and antidromically stimulated HVC_{RA} or HVC_X axon collaterals (Fig. 3). Antidromic stimulation of HVC_{RA} axon collaterals routinely elicited excitatory and inhibitory synaptic currents in HVC_{Av} neurons (Fig. 3a, left inset; EPSC: 10/11 cells; IPSC: 9/11 cells (Supplementary Fig. 3); no input: 1/11 cells; 5 birds). In contrast, antidromic stimulation of HVC_X cells never evoked a synaptic response in HVC_{Av} neurons (Fig. 3a, right inset; 0/8 cells; 4 birds), even though the same stimulation could elicit antidromic spikes in HVC_X neurons (Fig. 3b, right inset; n = 2/5 cells; 2 birds) and also evoked synaptic responses in both HVC_{RA} (Fig. 3b, left inset; EPSC: 2/5 cells; IPSC: 2/5 cells; no input: 1/5 cells; 3 birds) and HVC_X neurons (Supplementary Fig. 3; IPSC: 3/5 cells; no input: 0/5 cells; 2 birds). Furthermore, although axons from two of HVC's afferents, the thalamic nucleus Uva and the telencephalic nucleus interface (NIf), enter HVC along its rostroventral border, electrical stimulation along this border failed to evoke synaptic responses in HVC_{Av} neurons (Supplementary Fig. 3; n = 0/8 cells; 4 birds). Therefore, HVC_{Av} neurons are specifically positioned within the HVC microcircuit to convey song timing information from HVC_{RA} neurons to the auditory system.

Genetically ablating HVC_{Av} neurons disrupts juvenile song copying

Juvenile male zebra finches memorize a tutor song between 20 and 60 days after hatching and then copy this memorized song model in a process of sensorimotor learning that spans from 45 to 90 days [15,17]. To determine the role of HVC_{Av} neurons in song copying, we used an intersectional genetic method [42] to selectively ablate these cells in juvenile birds after they had an opportunity to memorize a tutor song, but before they had formed an accurate copy of the tutor song model (Fig. 4a, b). We injected a virus expressing a Cre-dependent form of caspase 3 (AAV2/1-FLEX-taCasp3-TEVp), which triggers cellular apoptosis [42], into HVC and injected a retrogradely transported virus expressing Cre-recombinase (AAV2/9-CMV-Cre) into Av of juvenile male zebra finches (Fig. 4a,b; n = 5 male zebra finches; 35–40d when injected with viruses; viral expression required 2–4 weeks (see Methods)). Siblings that received either no virus or that were injected only with AAV2/1-FLEX-taCasp3-TEVp into HVC served as control groups. To quantify the effects of this cell killing method we injected a retrograde tracer into Av in adult birds that had been subjected to

intersectional HVC_{Av} lesions as juveniles and quantified the number of surviving HVC_{Av} neurons. Intersectional expression of Cas3 in HVC_{Av} neurons of juveniles significantly reduced the adult number of HVC_{Av} neurons compared to either of two control groups (Fig. 4c; the two control groups had similar numbers of HVC_{Av} neurons and were subsequently treated as a single group).

All birds were raised to adulthood and their adult songs were compared to their tutors' songs to quantify song copying (see Methods). Genetically ablating HVC_{Av} neurons in juveniles severely disrupted their ability to copy a tutor song (Fig. 4 d–e; n = 5 experimental birds, 46.3% similarity to tutor song; n = 8 control siblings, 72.9% similarity; Mann-Whitney U = −3.8, Z = 2.56, $P = 0.01$). Within-bird comparisons indicated that similarity of the adult pupil's song to the tutor song correlated with the number of surviving HVC_{Av} neurons in the pupil's brain (Fig. 4 f–h). Most pupils were able to copy at least some syllables from their tutor (Fig. 4e and g, Supplementary Fig. 4, 4/5 birds copied at least one syllable from their tutor, with syllable copying determined by >70% accuracy, see Methods), suggesting that reducing the numbers of HVC_{Av} neurons does not block the capacity or motivation to copy individual syllables. Nonetheless, lesioned birds as a group failed to faithfully copy their tutors, indicating that HVC_{Av} neurons are necessary to normal levels of song copying.

A remaining issue is whether the song copying deficits resulted from ablating HVC_{Av} neurons, and not to the incidental cell death of other HVC neurons. In a separate group of birds, we tested whether the intersectional methods used to target HVC_{Av} cells also kill HVC_X cells, some of which extend axons through or near Av and might plausibly take up the AAV 2/9 Cre virus from the injection site in Av. However, we found that the number of HVC_X neurons was unaffected by the intersectional method used to kill HVC_{Av} neurons (Supplementary Fig. 5; n = 2 birds; see Methods). Therefore, deficits in song copying most likely arise from the selective loss of HVC_{Av} neurons.

Ablating HVC_{Av} neurons protects song's temporal features in deafened adults

Adult zebra finches use auditory feedback to maintain stable songs, as deafening triggers spectral degradation of individual syllables and also destabilizes syllable sequences over a period of days to weeks [43]. Furthermore, much of the neural circuitry implicated in song copying in juveniles also plays a role in feedback-dependent song maintenance in adults. For example, lesions placed in LMAN, the premotor output of a cortico-basal ganglia pathway important to juvenile song learning, have little effect on adult song but largely prevent deafening-induced song degradation [44]. To test whether HVC_{Av} neurons are also important to song maintenance, we first selectively ablated HVC_{Av} neurons in adult zebra finches and recorded their songs for six to ten weeks. All birds continued to sing highly stereotyped songs following ablation of HVC_{Av} neurons (Fig. 5a, b; two-sample $t(22) = -1.4$, $P = 0.16$ for HVC_{Av} - lesioned birds (n = 12) versus HVC_{Av} intact birds (n = 12)). Although there was a slight yet significant decrease in song self-similarity and motif duration (Supplementary Fig. 6), the trial-to-trial variability in spectral features of individual syllables and timing of inter-syllable gaps were unaffected by bilateral ablation of HVC_{Av} neurons (syllable frequency: two-sample paired $t(4) = 0.2$, $P = 0.8$; inter-syllable gaps: two-sample paired $t(4) = 1.3$, $P = 0.27$; n = 5 birds in each group). In contrast, unilateral HVC lesions,

made by injecting AAV2/1-FLEX-taCasp3-TEVp and AAV2/9-CMV-Cre into HVC, disrupted song production in a manner similar to the effects of unilateral HVC lesions (Supplementary Fig. 4) [45]. In summary, in adult birds with intact hearing, selectively ablating HVC_{Av} neurons exerted little effect on acute song performance, trial-to-trial song variability, or longer-term song maintenance.

We then deafened a cohort of adult male zebra finches in which we had previously bilaterally ablated HVC_{Av} neurons and also deafened another cohort of animals in which HVC was left intact (n = 7 animals in each group). Visual inspection of sonograms suggested that the songs of birds with HVC_{Av} lesions remained more stable following deafening than the songs of deafened birds with an intact HVC (Fig. 5c). To better characterize these contrasting effects, we quantified temporal changes by calculating differences in syllable transition matrices generated before and 10 weeks after deafening and quantified spectral changes using a self-similarity score over the same period (Fig. 5d, e; see Methods). Selectively ablating HVC_{Av} neurons largely prevented deafening-induced destabilization of syllable sequences, as revealed by lower differences in matrix scores in deafened birds with HVC_{Av} lesions (Fig. 5d, e) (two-sample $t(12) = -4.8$, $P = 0.0004$ for changes in song syllable transition matrix before and after deafening from seven lesioned versus seven intact birds). In contrast, HVC_{Av} lesions did not prevent spectral degradation of syllables following deafening, as self-similarity scores before and 10 weeks after deafening were similar in the experimental and control groups (Fig. 5e; two-sample $t(12) = 1.9$, $P = 0.07$ comparing self-similarity scores from HVC_{Av} - lesioned versus control birds). Indeed, in birds with HVC_{Av} lesions, within-syllable comparisons before and after deafening revealed significant increases in entropy, a measurement highly sensitive to song's spectral features (Fig. 5f; Supplementary Fig. 6; two-sample $t(11) = -4.0$, P = 0.0019 for changes in entropy measured in single syllables in HVC_{Av} - lesioned birds before and 10 weeks after deafening). Thus, ablating HVC_{Av} neurons protects temporal but not spectral features of song from deafening-induced degradation, consistent with the idea that these neurons serve a specialized role in mediating feedback-dependent changes to song timing.

A role for HVC_{Av} neurons in song timing plasticity

To further explore the role of HVC_{Av} neurons in feedback-dependent song plasticity, we used singing-contingent playback of white noise to induce adult birds to modify either the spectral (i.e., fundamental frequency, or "pitch") or temporal (i.e., song element duration) features of their songs before and after bilaterally ablating HVC_{Av} neurons. These experiments exploit slight trial-to-trial variations in syllable pitch and song element timing: targeting white noise playback to pitch or timing variants that fall above or below a user-set threshold drives the bird to adaptively modify pitch or timing, subsequently reducing the number of renditions that trigger noise playback. Notably, adult finches can independently modify either syllable pitch or song element duration using these protocols and also rapidly recover their original pitch and timing once noise playback is discontinued [16,18].

We measured rates of pitch and song element duration learning and subsequent recovery before and after genetic ablation of HVC_{Av} neurons. Rates of pitch learning and recovery did not differ before and after genetic ablation of HVC_{Av} neurons (Fig. 6a–c, n = 5 birds). In

contrast, almost all (4/5) birds in which HVC_{Av} neurons were ablated displayed much slower rates of song element duration learning and all (5/5) were severely impaired in their ability to recover their original song element timings after noise playback was discontinued (Fig. 6d–f). Taken together with the adult deafening studies, these findings indicate that HVC_{Av} neurons play a specialized role in the feedback-dependent modification and recovery of song timing in adult zebra finches.

DISCUSSION

This study identifies a previously unknown neuron type in the song nucleus HVC that transmits vocal motor-related signals to the auditory system and that plays an important role in juvenile and adult forms of vocal learning. These HVC_{Av} neurons form the cellular linchpin of a vocal premotor to auditory microcircuit: they are privileged synaptic targets of HVC_{RA} cells, which generate premotor signals important to song timing [20,24,25,35] and they transmit information to Avalanche, a discrete nucleus in the caudal mesopallium (CM), a part of the avian secondary auditory cortex [29]. Because CM is reciprocally connected with other auditory regions implicated in song learning [46,47], the HVC to Av synapse may afford a crucial site where vocal motor-related signals interact with the auditory system to affect song learning and maintenance.

The anatomical placement of the HVC_{Av} neuron in the sensorimotor hierarchy of the songbird brain is reminiscent of motor cortical to auditory cortical projections in the mammalian brain. In the mammalian brain, these motor cortical inputs provide a source of movement-related signals that can suppress and modulate auditory processing in a state- and movement-dependent manner [1,2,23,48]. In humans, projections from speech production regions in the frontal cortex to the auditory cortex are theorized to serve various roles, including the suppression of vocalization-related auditory feedback, the segregation of reafferent from exafferent acoustical stimuli and, in a related vein, the generation of forward interactions speculated to facilitate speech learning and maintenance [6,8]. The location of HVC_{Av} cells in the motor to sensory arc and their role in juvenile song copying and adult modification of song timing are consistent with a forward circuit important to vocal learning.

The current findings support the idea that HVC_{Av} cells transmit motor-related signals to the auditory system that are important for learning and modifying song timing. First, HVC_{Av} cells receive input from HVC_{RA} cells, which are a source of premotor signals for song timing [20,24,25], but do not appear to receive input from HVC_{X} cells or from either Uva or Nif, two afferents that convey motor- and auditory-related signals to HVC. This privileged organization could enable HVC_{Av} cells to provide a direct source of song timing information to the auditory system. Second, we found that selectively ablating HVC_{Av} neurons in juveniles markedly interferes with song imitation, while partially sparing their ability to copy individual syllables. Similarly, killing these cells in adults strongly impeded deafening-induced degradation of song's temporal features even though spectral degradation following deafening was still evident. Finally, most adults with reduced numbers of HVC_{Av} cells displayed slower rates of song element duration learning, and all of them failed to recover normal song timing following vocalization-contingent feedback perturbation. Together, these observations support the idea that HVC_{Av} cells are important to the learning and

modification of song timing but not to pitch learning, two processes that prior studies indicate are mediated by distinct neural pathways [16,28]. Therefore, functional dissection of circuits downstream of the HVC_{Av} cell may help identify mechanisms that underlie the learning and feedback-dependent modification of vocal timing.

The region immediately downstream of HVC_{Av} cells - Avalanche - is embedded in CM, a part of the avian secondary auditory cortex that contains a variety of distinct neuron types, including some that exhibit evidence of song-related corollary discharge [22]. The placement of HVC_{Av} cells in the motor to sensory hierarchy and their motor-related activity during singing makes them a likely source of these corollary discharge signals [22,24]. Notably, a key function of corollary discharge signals in forward models of sensorimotor integration is to help generate error signals important to learning and maintaining skilled behaviors [6–9]. In fact, neurons that detect errors in singing-related auditory feedback exist in CM and other regions of the songbird auditory forebrain and may receive indirect input from HVC_{Av} cells [22,49]. Finally, some neurons in these downstream auditory regions innervate midbrain dopaminergic neurons [49,50], which are speculated to generate error correction signals that drive adaptive vocal plasticity in both juvenile and adult songbirds. Therefore, a pathway involving relatively few synapses may enable motor-related signals emanating from HVC to influence error detection and error correction processes necessary to vocal learning.

In this light, it is worthwhile to contrast the effects of selective HVC_{Av} cell ablation with lesions made in LMAN, the output nucleus of the cortico-basal ganglia pathway. Although both types of lesions disrupt juvenile song copying and slightly shorten motif duration, LMAN lesions in adults block pitch learning but do not severely interfere with noise-contingent modulation or recovery of song timing [16], whereas HVC_{Av} cell lesions interfere with the modification and recovery of song timing but leave pitch learning and recovery unaffected. Another notable difference is that HVC_{Av} cell lesions selectively preserve song's temporal features following adult deafening, whereas LMAN lesions block deafening-induced degradation of song's spectral and temporal features [44]. Thus although both HVC_{Av} and LMAN lesions provide some protection from deafening-induced song degradation, these protective effects may result from disruptions at different stages of sensorimotor processing. Specifically, we speculate that HVC_{Av} lesions attenuate deafening-induced song degradation by reducing the strength of motor-based signals necessary to error detection, thus minimizing the strength of error signals that would normally arise in the absence of singing-related auditory feedback. In contrast, LMAN lesions occlude deafening-induced changes by preventing these error signals from engaging the error correction machinery in the cortico-basal ganglia network.

An important goal of future studies will be to analyze the circuit computations that result from interactions between HVC_{Av} neurons and downstream neurons in the auditory forebrain. One possibility is that motor-related signals from HVC_{Av} neurons gate transmission from the auditory forebrain to HVC in a vocalization-dependent manner. Consistent with this idea, auditory inputs to HVC are rapidly gated "off" during singing and some auditory neurons in CM display reduced sensitivity to auditory stimulation during vocalization [22,38]. Another related possibility is that vocal motor-related signals from HVC to the auditory system function as part of a predictive mechanism, as theorized to occur in

forward models of vocal learning [5,6,8]. In this scenario, HVC_{Av} neurons transmit a corollary discharge signal to the auditory system that is shaped by prior vocal experience to predict features of auditory feedback that are a consequence of HVC's premotor activity. Circuits downstream of HVC that integrate such predictive signals with vocalization-related feedback could give rise to the putative error signals that have been detected in CM and other parts of the auditory forebrain. Of course, song learning depends not only on the individual's experience of his vocalizations but also on auditory experience of an appropriate song model, the latter of which is stored as a long term auditory memory. Thus, a distinct possibility is that vocalization-dependent signals transmitted by HVC_{Av} neurons to the auditory system reactivate this song memory in a context-dependent manner and temporally register it with vocalization-related auditory feedback, facilitating the comparisons between song memories and song performance that are necessary to vocal learning.

Methods

Juvenile and adult male zebra finches were obtained from the Duke University Medical Center and the UT Southwestern Medical Center breeding facilities. Experimental procedures were conducted in accordance with the National Institutes of Health guidelines and were reviewed by the Duke University Medical Center and UT Southwestern Medical Center Animal Care and Use Committees.

Anatomical pathway tracing and cell counts

Juvenile and young adult zebra finches (60–140 d) were anesthetized with 2% isofluorane gas before placing them in a custom stereotaxic apparatus. After applying a topical anesthetic (0.25% bupivacaine) and making a vertical incision in the skin over the skull, ~1 mm craniotomies were made in the skull at a predetermined distance from the bifurcation of a major blood vessel ('y-sinus'; Av: 1.75mm anterior, 2.0mm lateral, 1mm deep; RA: 1.0mm posterior, 2.4mm lateral, 2.0–2.5mm deep; Area X:, 5.1mm anterior, 1.6mm lateral, 3.0mm deep). Using a glass pipette attached to a pressure injection system (Drummond Nanoject II), bilateral injections of AlexaFluor dextrans 594 or 488 (10,000 MW; Life Technologies), Fast blue (Sigma or Polysciences; 3 injections of 32.2 nl) or virally-encoded GFP (AAV2/9.CMV-scGFP, PennVector; 30 injections of 32.2 nl) were made into Av, RA and/or Area X. After tracer injections, craniotomies were sealed with bone wax and the incision site in the skin closed with a tissue adhesive (VetBond). After 6 days, or one month in the case of viral injections, birds were deeply anesthetized with an I.P. injection of pentobarbital solution (Euthasol) and perfused with 0.025 M phosphate-buffered saline followed by 4% paraformaldehyde. The brain was removed and placed in a cryoprotective formalin sucrose solution overnight and serially cut on a freezing sliding microtome into 50 um-thick consecutive sagittal sections. Sections containing HVC were mounted onto glass slides, coverslipped with Fluoromount-G. All retrogradely-labeled HVC_{Av} neurons were then counted under a fluorescent microscope (Zeiss Axioskop).

Whole-cell recordings from HVC neurons

Targeted whole-cell recordings were made from retrogradely labeled HVC neurons in zebra finches (38–72 d). Sagittal brain slices of 300 μm thickness were prepared with a vibratome

(VT1000S, Leica) in cutting solution containing (mM): 238 sucrose, 2.5 KCl, 26.2 $NaHCO_3$, 1 NaH_2PO_4, 11 dextrose, and 3.8 $MgCl_2$. The slices were stored briefly at 35°C and then at room temperature before transferred into recording chamber. Recordings were made at ~30°C in ACSF containing (mM): 119 NaCl, 2.5 KCl, 26.2 $NaHCO_3$, 1 NaH_2PO_4, 11 dextrose, 1.3 $MgCl_2$, and 2.5 $CaCl_2$, equilibrated with 95% O_2/5% CO_2. For recordings of spikes in HVC neurons, pipette solution contained (mM): 124 K-gluconate, 4 NaCl, 10 HEPES, 2 EGTA, 2 $MgCl_2$, 2 ATP-Mg, 0.3 GTP-Na_3, 10 phosphocreatine-Na_2, and 0.05 Alexa 594 hydrazide (pH 7.3, adjusted with KOH). For recordings of EPSCs in HVC_{Av} neurons, the pipette solution contained (mM): 120 Cs-methanesulfonate, 4 NaCl, 10 HEPES, 2 EGTA, 2 $MgCl_2$, 2 ATP-Mg, and 0.3 GTP-Na_3, 10 phosphocreatine-Na_2, 5 QX-314 bromide, and 0.05 Alexa 594 hydrazide. (pH 7.3, adjusted with CsOH). The pipettes were fabricated from borosilicate glass and the pipette resistance was 5 – 8 MΩ. Membrane potentials were corrected for measured liquid junction potentials just before each recording.

Data were acquired with Multiclamp 700B, low-pass filtered at 2.8 kHz, and digitized at 20 kHz. Recordings with high series resistance of > 30 MΩ or a large leak current (the resting current of < −100 pA at −70 mV) were excluded from the analysis. The series resistance was compensated by 30%. At the beginning of recordings, 500 ms voltage pulses from −70 mV to −90 mV were applied to measure input resistance and I_h amplitude. The I_h amplitude was estimated as the difference between current responses during 80–100 ms and 480–500 ms after the pulse onset. To characterize firing properties of HVC neurons, 500 ms current pulses were applied from the resting current of 0 pA. Spike adaptation was quantified as the difference between the first and last inter-spike-interval at the mean firing rate of ~40 Hz. Spike gain was calculated as a slope of a line fit to the firing rate-current relation (Hz/nA) in the range of < 40 Hz. To examine synaptic connections from HVC_{RA} to HVC_{Av} neurons, HVC_{RA} axons were antidromically stimulated with a concentric bipolar electrode (CBBRC75; FHC) placed midway between HVC and RA and evoked EPSCs were recorded in HVC_{Av} neurons voltage-clamped at −70mV.

Genetic ablation of HVC_{Av} neurons

Using a similar procedure to that described above for tracer injections, we anesthetized zebra finches (35–40 d for juvenile experiments, 105–110 d for adult experiments) and placed them in a stereotaxic apparatus. After making an incision in the skin, we made craniotomies over Av and HVC at predetermined distances from the y sinus (Av: 1.75mm anterior, 2.0mm lateral, 1mm deep; HVC: 2.4mm lateral, 0.375mm deep). To selectively ablate HVC_{Av} cells, we made bilateral injections of a retrogradely transported Cre construct (AAV2/9.CMV.HI.GFP-Cre.SV40; Penn Vector) into Av and a locally expressed Cre-dependent caspase construct (AAV2/1.Ef1α.FLEX-Casp3-2A-TEV; Nirao Shah, UCSF) into HVC (13 injections of 32.2 nl of Cre, 28 injections of 32.2 nl of CS3). After injections, craniotomies were sealed with bone wax, the incision site closed with VetBond and birds were allowed to recover from anesthesia under a heat lamp. Birds were injected with AlexaFluor 594 dextrans into Av 6 days prior to perfusion and HVC_{Av} cell numbers were quantified by counting all retrogradely labeled HVC_{Av} neurons in HVC. To examine if viral HVC_{Av} lesions inadvertently killed HVC_X cells, some of which extend axons through or near Av, we made bilateral injections of retrogradely transported Cre into Av and unilateral

injections of locally expressed Cre-dependent caspase virus into HVC. Birds were then injected with AlexaFluor 594 dextrans into Area X 6 days prior to perfusion and HVC_X cell numbers were quantified by counting all retrogradely labeled HVC_X neurons in HVC.

Bilateral removal of cochlea

Adult male birds (100–140 d) were anesthetized with Equithesin and secured to a custom-made metal platform. The tympanic membrane and inner ear bones occluding the oval window were removed with forceps and the cochlea was removed with a small wire hook. Cochleas were then examined under the dissecting microscope to ensure complete removal. The incision site in the skin was closed with VetBond and birds recovered from anesthesia under a heat lamp.

Calcium Imaging of HVC_{Av} Neurons

Using similar surgical procedures as those described in the ablation experiments above, we made bilateral injections of either a retrogradely transported GCaMP (AAV2/9.CAG.GCaMP6s; Penn Vector) into Av (54 injections of 9.2 nl of GCaMP, n = 3 birds) or a retrogradely transported Cre (AAV2/9.CMV.HI.GFP-Cre.SV40; Penn Vector) into Av (43 injections of 9.2 nl of Cre) and a locally expressed Cre-dependent GCaMP6s construct (AAV2/1.FLEX.CAG.GCaMP6s; Penn Vector) into HVC (54 injections of 9.2 nl of GCaMP, n = 1 bird). Three weeks after viral injection birds were injected with Alexa Fluor 594 dextrans into Area X to help visualize HVC. Four weeks after viral injection the skull and dura over HVC were removed and Kwik-Sil (World Precision Instruments) was placed over the putative site of HVC. The bird was then imaged under an epifluorescence microscope (Zeiss 510) to determine the borders of HVC by the presence of 594 dextrans in HVC_X cells. A 1 mm diameter Gradient-Index (GRIN) lens was then implanted on the dorsal surface of HVC within the identified boundaries. Next, a baseplate was implanted on the bird's skull to hold a miniature microscope (Inscopix, nVista HD) for imaging. After a period of recovery (~3 days), birds were placed in a recording chamber and the miniature microscope was attached to the baseplate for imaging. The activity of HVC_{Av} neurons was then imaged and data was collected using nVista software (Inscopix) (fluorescence) and a custom written acquisition program in LabVIEW (sound and frame times). The LED power was maintained between 10 and 20 percent, corresponding to 0.12 and 0.24 mW/mm2. The maximum field of view was 1440 pixels x 1080 pixels; 900 μm x 650 μm. Pixel size was 0.625 by 0.625 μm. Sound was sampled at 44 kHz and imaging data were sampled between 10Hz and 30Hz corresponding to exposure time of 99.84 ms to 33.25 ms. Imaging data acquired above 10Hz were down sampled such that all analyses were performed on 10Hz signals. Imaging sessions were conducted in 30 second trials in which LED power was on and data were recorded. Offline analysis of imaging data was performed using Mosaic (Inscopix) and custom software written in MATLAB. Change in fluorescence in the raw imaging data was quantified with $\Delta F/F0$ calculated as $(F-F0)/F0$. Next, Regions of Interest (ROIs) were manually drawn containing a large fraction of the brain surface (defined as 'bulk signal') or in cases where signals resembling cells could be identified, a modified CNMF algorithm adapted for single photon microendoscope data [39] was used to automatically identify ROIs corresponding to putative individual neurons. Fluorescence traces for both bulk signals and putative single neurons were computed and then aligned to

audio recordings of song. Song bouts were identified by visual inspection and were defined as sequences of introductory notes and syllables separated by gaps of less than 0.5 s. Song onset was defined as the first frame after the onset of the first element of song and song offset as the first frame after the offset of the last element of song. Mean fluorescence responses related to singing were computed by averaging the bulk signal responses of every song bout before (n = 49 songs from 4 birds) and after deafening (n = 30 songs from 2 birds). In one control bird the same procedures were performed in the absence of viral injection (n = 10 songs from 1 bird).

Behavioral analysis of song learning and song stability

Percentage similarity score, accuracy and sequential match scores in SOUND ANALYSIS PRO were used to quantify the similarity of the pupil's song to that of its tutor in our juvenile CS3 experiments (http://soundanalysispro.com/manual-1/chapter-10-similarity-measurements/the-similarity-score). The %similarity score compares large scale features of songs measured over 50–70 ms time windows by calculating Euclidean distances across mean values of song spectral features (pitch, FM, AM, Wiener entropy, and goodness of pitch). This score reflects the percentage of the tutor's song that has been copied by the pupil. The accuracy score provides a measure of the local similarity of the pupil song to the tutor song as calculated over 5–10 ms time windows. The sequential match score provide a measure of how well the sequence of the tutors song was copied by comparing the temporal ordering of the 50–70ms time windows in the tutor's song to those in the pupil's song with an 80 ms alignment tolerance. We also used % similarity to quantify the similarity of the bird's song after CS3/Cre viral injection to its song before injection in our adult CS3 experiments.

In song learning experiments juveniles injected with AAV2/9.CMV.HI.GFP-Cre.SV40 in Av and AAV2/1.Ef1α.FLEX-Casp3-2A-TEV in HVC, and control siblings, including those injected with AAV2/1.Ef1α.FLEX-Casp3-2A-TEV alone in HVC and those not receiving any viral injections, were housed with their father until 60 days of age, at which point birds were raised in isolation until adulthood (90–100 days). To determine the similarity of the pupil's song to the tutor's song, we calculated similarity scores by comparing the adult pupil's song (90–100 d) to the song of their tutor (n > 30).

In adult HVC_{Av} ablation experiments, we recorded songs 1–2 days before viral injections then again ~4 weeks after injection with AAV2/9.CMV.HI.GFP-Cre.SV40 in Av and AAV2/1.Ef1α.FLEX-Casp3-2A-TEV in HVC. A subset of these birds was subsequently deafened and their songs recorded 10 weeks later. We calculated baseline similarity scores to establish that the bird sang a relatively stable song before injection by comparing pairs of motifs before injection (n > 30 motif pairs). We then compared pairs of motifs before and after injection (n > 30motif pairs) to determine if the bird's song changed after HVC_{Av} lesions. For the subset of deafened birds, motifs were compared immediately before and 10 weeks following deafening (n > 30).

To examine sequential changes in song syllable structure of deafened birds, we quantified changes in transitions from one song syllable to the next. Using custom written scripts (Matlab) we classified individual syllables and calculated the probability of transition from

one syllable to the next. After assembling a matrix of all syllable transitions for songs before deafening and after deafening, we subtracted the post-deafening matrix from the pre-deafening matrix. The difference matrix score was calculated by taking the average of the transition probabilities along the top left-to-bottom right diagonal of the difference matrix, which corresponds to the core syllable transition sequence of the bird's song. The resulting "difference matrix" was used to examine the change in transition probability after deafening. For example, before deafening a bird sings "A B C" with a 100% probability that B follows A, a 100% probability that C follows B, and a 100% probability that the end of the sequence follows C. These three probabilities lie along the left top to bottom right diagonal of the transition matrix and correspond to the core syllable transition sequence of the bird's song. If after deafening the probability that B would follow A was reduced from 100% to 50%, we would take the difference of the probability that B would follow A before deafening and probability that B would follow A before deafening (i.e. $P(A|B)_{before} - P(A|B)_{after} = P(A|B)_{\text{difference matrix score}}$). We would then average the difference matrix scores from each transition to arrive at the overall difference matrix score (i.e. mean [$P(A|B)_{\text{difference matrix score}}$ $P(B|C)_{\text{difference matrix score}}$ $P(C|end)_{\text{difference matrix score}}$. The lower the overall difference matrix score, the less the bird's core syllable sequence changed after deafening.

Song Feature Modulation

A modified version of the Conditional Auditory Feedback software (LabVIEW) by Ali et. al. was used to implement the song feature modulation protocol. Real-time auditory input from the bird's cage is input to the program which then takes measurements (e.g. duration or pitch) on a targeted region of the bird's song as it is sung. Detection is done by comparing auditory input to a template, a sound file containing a recording of a portion of the bird's song (150–500ms in length) that immediately precedes the desired target region. For pitch modulation, targeted regions were 5ms components of the bird's song that had a well-defined pitch (i.e. harmonic stack). For timing modulation, targets were the region between the onset of two syllables, i.e. they included a syllable + an intersyllable gap and ended at the start of the next syllable. Targets were chosen where onsets of the two syllables were well-defined with clear rapid rises in amplitude. This is the 'song element' referred to the in paper. Targets, for both pitch and timing modulation, also needed to be preceded by a sufficient amount of song to create a template allowing for detection with high sensitivity and specificity. Throughout all experiments we estimated that the true detection rate (# of measurements of the intended target / # of times target produced) remained above 75%. We also estimate that the false measurement rate (# of measurements of unintended regions / # of measurements made) remained below 25%. Modulation of the bird's song was then achieved by the playback of white noise into the bird's chamber whenever the measurement of the target region fell below a set threshold value (in all experiments we drove the measurement 'up'). Initial threshold values were set at the average value of the measurement recorded over a 3 day baseline period. Threshold values were then dynamically adjusted by the program as the bird altered its song: whenever 80% of the last 200 measurements were above the threshold, the threshold was then set to the mean of the last 200 measurements, though only if this mean was above the current threshold.

The experimental protocol was as follows: Adult birds were initially injected bilaterally into Av with AAV2/9-Cre-GFP. Birds were then run through either pitch or timing modulation protocols. Before starting white noise, baseline measurements of the target were calculated over at least a 3 day period. White noise was then turned on to drive the value of the measurement up and was kept on until the daily average value of the measurement was at least 2 standard deviations higher than the average value of the measurement over the baseline period. The standard deviation used here was the standard deviation of the measurements over the baseline period. Birds were then allowed to return passively (white noise turned off). 3 birds were then run through the protocol again, but now to modulate the other feature (i.e. if they had just run through pitch modulation they were now run through timing modulation). 2 birds only did timing modulation and 2 birds only did pitch modulation. After returning to baseline, birds were then injected with AAV2/1 flex-taCas3-TEVp into HVC bilaterally. Birds were then given at least 3 weeks before starting the next arm of the experiment. Birds were then again run through whichever feature modulation protocols they had done previously. Post-caspase injected birds did not have clear returns to baseline for timing features so they were allowed to return (passive measurements) for as many days as they required pre-caspase injection + an extra 5–10 days.

Statistical Analysis

Male zebra finches were randomly assigned to experimental groups. No statistical methods were used to pre-determine sample sizes but our sample sizes are similar to those reported in previous publications [16,19,25]. Datasets used for statistical comparisons were tested for normality and none of the data were excluded from analysis. Parametric (two-tailed two-sample t-test and paired t-tests) or nonparametric tests (Mann-Whitney U test) were used accordingly for statistical comparisons. Data collection and analysis were not performed blind to the conditions of the experiments. A Supplementary Methods Checklist is available.

Data Availability

The data that support the findings of this study, and any associated custom software used in data analysis, are available from the corresponding authors upon reasonable request.

Code Availability

Song feature modulation code for pitch and temporal learning of song and analysis code for population calcium imaging data have been previously published [16,39]. LabVIEW codes for acquisition of imaging frames and sound for calcium imaging experiments is included in Supplemental Software.

Supplementary Material

Refer to Web version on PubMed Central for supplementary material.

Acknowledgments

The authors thank Drs. David Schneider, Katherine Tschida, Timothy Warren, and Stephen Lisberger for reading and commenting on the manuscript, K. Hamaguchi (Duke University Medical Center) for software support, J. Baltzegar, M. Booze (Duke University Medical Center), J. Holdway and A. Guerrero (UT Southwestern Medical

Center) for animal husbandry and laboratory support. This research was supported by grants from the National Science Foundation (R.M. (IOS-1354962), T.F.R. (IOS-1457206, IOS-1451034)); the US National Institutes of Health (R.M. (R01DC002524, R01NS099288), T.F.R (R01DC014364), N.M.S. (R01NS049488, R01NS083872)); an Inscopix DECODE Award (R.M.); the Klingenstein-Simons Fellowship (T.F.R.); the Ellison Medical Foundation (N.M.S.); a JSPS Postdoctoral Fellowship for Research Abroad (M.T.); an Alpha Omega Alpha Research Fellowship (G.C.) and a NARSAD Young Investigator Grant (Essel Investigator) from the Brain & Behavior Research Foundation (T.F.R.).

References

1. Eliades SJ, Wang X. Neural substrates of vocalization feedback monitoring in primate auditory cortex. Nature. 2008; 453:1102–1106. DOI: 10.1038/nature06910 [PubMed: 18454135]
2. Schneider DM, Nelson A, Mooney R. A synaptic and circuit basis for corollary discharge in the auditory cortex. Nature. 2014; 513:189–194. DOI: 10.1038/nature13724 [PubMed: 25162524]
3. Lee S, Kruglikov I, Huang ZJ, Fishell G, Rudy B. A disinhibitory circuit mediates motor integration in the somatosensory cortex. Nat Neurosci. 2013; 16:1662–1670. DOI: 10.1038/nn.3544 [PubMed: 24097044]
4. Niell CM, Stryker MP. Modulation of visual responses by behavioral state in mouse visual cortex. Neuron. 2010; 65:472–479. DOI: 10.1016/j.neuron.2010.01.033 [PubMed: 20188652]
5. Wang J, et al. Action planning and predictive coding when speaking. Neuroimage. 2014; 91:91–98. DOI: 10.1016/j.neuroimage.2014.01.003 [PubMed: 24423729]
6. Hickok G, Houde J, Rong F. Sensorimotor integration in speech processing: computational basis and neural organization. Neuron. 2011; 69:407–422. DOI: 10.1016/j.neuron.2011.01.019 [PubMed: 21315253]
7. Crapse TB, Sommer MA. Corollary discharge across the animal kingdom. Nat Rev Neurosci. 2008; 9:587–600. DOI: 10.1038/nrn2457 [PubMed: 18641666]
8. Houde JF, Chang EF. The cortical computations underlying feedback control in vocal production. Curr Opin Neurobiol. 2015; 33:174–181. DOI: 10.1016/j.conb.2015.04.006 [PubMed: 25989242]
9. Cullen KE. Sensory signals during active versus passive movement. Curr Opin Neurobiol. 2004; 14:698–706. DOI: 10.1016/j.conb.2004.10.002 [PubMed: 15582371]
10. Sperry RW. Neural basis of the spontaneous optokinetic response produced by visual inversion. J Comp Physiol Psychol. 1950; 43:482–489. [PubMed: 14794830]
11. Poulet JF, Hedwig B. The cellular basis of a corollary discharge. Science. 2006; 311:518–522. DOI: 10.1126/science.1120847 [PubMed: 16439660]
12. von Holst E, Mittelstaedt H. Das reaferenzprinzip [The prinicple of reafference]. Naturwissenschaften. 1950; 37:464–476.
13. Bell CC. An efference copy which is modified by reafferent input. Science. 1981; 214:450–453. [PubMed: 7291985]
14. Doupe AJ, Kuhl PK. Birdsong and human speech: common themes and mechanisms. Annu Rev Neurosci. 1999; 22:567–631. [PubMed: 10202549]
15. Immelmann, K. Bird Vocalisations. Hinde, RA., editor. Cambridge University Press; 1969. p. 61-74.
16. Ali F, et al. The basal ganglia is necessary for learning spectral, but not temporal, features of birdsong. Neuron. 2013; 80:494–506. DOI: 10.1016/j.neuron.2013.07.049 [PubMed: 24075977]
17. Eales LA. Song learning in zebra finches: some effects of song model availability on what is learnt and when. Anim Behav. 1985; 33:1293–1300.
18. Tumer EC, Brainard MS. Performance variability enables adaptive plasticity of ‘crystallized’ adult birdsong. Nature. 2007; 450:1240–1244. DOI: 10.1038/nature06390 [PubMed: 18097411]
19. Roberts TF, Gobes SM, Murugan M, Olveczky BP, Mooney R. Motor circuits are required to encode a sensory model for imitative learning. Nat Neurosci. 2012; 15:1454–1459. DOI: 10.1038/nn.3206 [PubMed: 22983208]
20. Long MA, Fee MS. Using temperature to analyse temporal dynamics in the songbird motor pathway. Nature. 2008; 456:189–194. [PubMed: 19005546]

21. Vallentin D, Kosche G, Lipkind D, Long MA. Neural circuits Inhibition protects acquired song segments during vocal learning in zebra finches. Science. 2016; 351:267–271. DOI: 10.1126/science.aad3023 [PubMed: 26816377]
22. Keller GB, Hahnloser RH. Neural processing of auditory feedback during vocal practice in a songbird. Nature. 2009; 457:187–190. DOI: 10.1038/nature07467 [PubMed: 19005471]
23. Heinks-Maldonado TH, Mathalon DH, Gray M, Ford JM. Fine-tuning of auditory cortex during speech production. Psychophysiology. 2005; 42:180–190. DOI: 10.1111/j.1469-8986.2005.00272.x [PubMed: 15787855]
24. Hahnloser R, Kozhevnikov A, Fee M. An ultra-sparse code underlies the generation of neural sequences in a songbird. Nature. 2002; 419:65–70. [PubMed: 12214232]
25. Hamaguchi K, Tanaka M, Mooney R. A Distributed Recurrent Network Contributes to Temporally Precise Vocalizations. Neuron. 2016; 91:680–693. DOI: 10.1016/j.neuron.2016.06.019 [PubMed: 27397518]
26. Alvarez-Buylla A, Kirn JR, Nottebohm F. Birth of projection neurons in adult avian brain may be related to perceptual or motor learning. Science. 1990; 249:1444–1446. [PubMed: 1698312]
27. Sohrabji F, Nordeen EJ, Nordeen KW. Selective impairment of song learning following lesions of a forebrain nucleus in the juvenile zebra finch. Behav Neural Biol. 1990; 53:51–63. [PubMed: 2302141]
28. Scharff C, Nottebohm F. A comparative study of the behavioral deficits following lesions of various parts of the zebra finch song system: implications for vocal learning. J Neurosci. 1991; 11:2896–2913. [PubMed: 1880555]
29. Akutagawa E, Konishi M. New brain pathways found in the vocal control system of a songbird. J Comp Neurol. 2010; 518:3086–3100. DOI: 10.1002/cne.22383 [PubMed: 20533361]
30. Mooney R. Different subthreshold mechanisms underlie song-selectivity in identified HVc neurons of the zebra finch. Journal of Neruoscience. 2000; 20:5420–5436.
31. Wild JM, Williams MN, Howie GJ, Mooney R. Calcium-binding proteins define interneurons in HVC of the zebra finch (Taeniopygia guttata). J Comp Neurol. 2005; 483:76–90. [PubMed: 15672397]
32. Dutar P, Vu HM, Perkel DJ. Multiple cell types distinguished by physiological, pharmacological, and anatomic properties in nucleus Hvc of the adult zebra finch. J Neurophys. 1998; 80:1828–1838.
33. Hattox AM, Nelson SB. Layer V neurons in mouse cortex projecting to different targets have distinct physiological properties. J Neurophysiol. 2007; 98:3330–3340. DOI: 10.1152/jn.00397.2007 [PubMed: 17898147]
34. Kim EJ, Juavinett AL, Kyubwa EM, Jacobs MW, Callaway EM. Three Types of Cortical Layer 5 Neurons That Differ in Brain-wide Connectivity and Function. Neuron. 2015; 88:1253–1267. DOI: 10.1016/j.neuron.2015.11.002 [PubMed: 26671462]
35. Long MA, Jin DZ, Fee MS. Support for a synaptic chain model of neuronal sequence generation. Nature. 2010; 468:394–399. DOI: 10.1038/nature09514 [PubMed: 20972420]
36. Liberti WA 3rd, et al. Unstable neurons underlie a stable learned behavior. Nat Neurosci. 2016; 19:1665–1671. DOI: 10.1038/nn.4405 [PubMed: 27723744]
37. Picardo MA, et al. Population-Level Representation of a Temporal Sequence Underlying Song Production in the Zebra Finch. Neuron. 2016; 90:866–876. DOI: 10.1016/j.neuron.2016.02.016 [PubMed: 27196976]
38. Hamaguchi K, Tschida KA, Yoon I, Donald BR, Mooney R. Auditory synapses to song premotor neurons are gated off during vocalization in zebra finches. Journal Article. 2014; 3:e01833.
39. Zhou P, Resendez SL, Stuber GD, Kass RE, Paninski L. Efficient and accurate extraction of in vivo calcium signals from microendoscope video data. 2016 arXiv:1605.07266v1 [q-bio.NC].
40. Prather JF, Peters S, Nowicki S, Mooney R. Precise auditory-vocal mirroring in neurons for learned vocal communication. Nature. 2008; 451:305–310. DOI: 10.1038/nature06492 [PubMed: 18202651]
41. Mooney R, Prather JF. The HVC microcircuit: the synaptic basis for interactions between song motor and vocal plasticity pathways. J Neurosci. 2005; 25:1952–1964. [PubMed: 15728835]

42. Yang CF, et al. Sexually dimorphic neurons in the ventromedial hypothalamus govern mating in both sexes and aggression in males. Cell. 2013; 153:896–909. DOI: 10.1016/j.cell.2013.04.017 [PubMed: 23663785]
43. Nordeen KW, Nordeen EJ. Auditory feedback is necessary for the maintenance of stereotyped song in adult zebra finches. Behav Neural Biol. 1992; 57:58–66. [PubMed: 1567334]
44. Brainard MS, Doupe AJ. Interruption of a basal ganglia-forebrain circuit prevents plasticity of learned vocalizations. Nature. 2000; 404:762–766. DOI: 10.1038/35008083 [PubMed: 10783889]
45. Williams H, Crane LA, Hale TK, Esposito MA, Nottebohm F. Right-side dominance for song control in the zebra finch. J Neurobiol. 1992; 23:1006–1020. DOI: 10.1002/neu.480230807 [PubMed: 1460461]
46. Fortune ES, Margoliash D. Parallel pathways and convergence onto HVc and adjacent neostriatum of adult zebra finches (Taeniopygia guttata). J Comp Neurol. 1995; 360:413–441. DOI: 10.1002/cne.903600305 [PubMed: 8543649]
47. Foster EF, Bottjer SW. Axonal connections of the high vocal center and surrounding cortical regions in juvenile and adult male zebra finches. J Comp Neurol. 1998; 397:118–138. [PubMed: 9671283]
48. Nelson A, et al. A circuit for motor cortical modulation of auditory cortical activity. J Neurosci. 2013; 33:14342–14353. DOI: 10.1523/JNEUROSCI.2275-13.2013 [PubMed: 24005287]
49. Mandelblat-Cerf Y, Las L, Denisenko N, Fee MS. A role for descending auditory cortical projections in songbird vocal learning. Journal Article. 2014; 3
50. Gale SD, Person AL, Perkel DJ. A novel basal ganglia pathway forms a loop linking a vocal learning circuit with its dopaminergic input. J Comp Neurol. 2008; 508:824–839. DOI: 10.1002/cne.21700 [PubMed: 18398824]

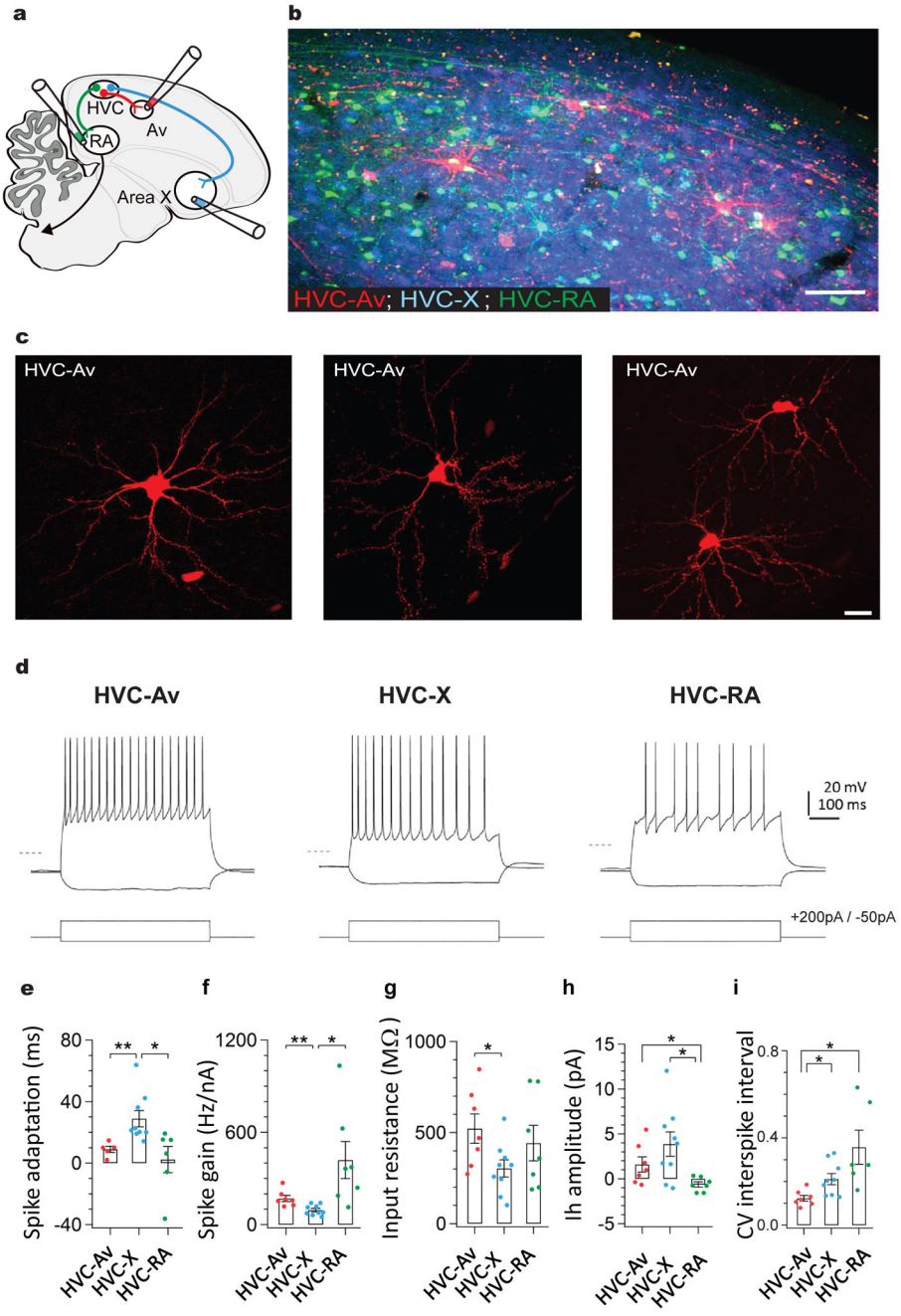

Figure 1. A distinct class of projection neurons links the song premotor nucleus HVC to the auditory region Avalanche

a) Schematic showing the design of retrograde labeling experiments. Different fluorescent retrograde tracers were injected into Av (dextran, Alexa Fluor 594), RA (dextran, Alexa Fluor 488), and Area X (fast blue). **b)** Parasagittal section through retrogradely labeled HVC (left panel) reveals that neurons projecting into Avalanche (red) are distinct from neurons projecting to Area X (blue) or RA (green). Inset shows magnified image outlined by white box. **c)** Images of individual HVC_{Av} neurons retrogradely labeled by AAV2/9 GFP injection into Av. **d)** Visualized whole-cell current clamp recordings from retrogradely-labeled HVC

projection neurons in brain slices in response to 500ms current injection (−50 and +200 pA; dashed line = −80mV). HVC_{Av} neurons differ from HVC_X neurons in their intrinsic properties, including their **e)** spike adaptation rate (two-sample $t(10) = 3.5$, $P = 0.005$ for HVC_{Av} neurons (n = 5) versus HVC_X neurons (n = 9); two-sample $t(9) = 2.6$, $P = 0.02$ for HVC_X neurons (n = 9) versus HVC_{RA} neurons (n = 6)), **f)** spike gain (two-sample $t(10) = 3.3$, $P = 0.007$ for HVC_{Av} neurons (n = 7) versus HVC_X neurons (n = 9); two-sample $t(6) = 2.7$, $P = 0.03$ for HVC_X neurons (n = 9) versus HVC_{RA} neurons (n = 7)), **g)** input resistance (two-sample $t(10) = 2.3$, $P = 0.04$ for HVC_{Av} neurons (n = 7) versus HVC_X neurons (n = 9)). **h)** HVC_{Av} neurons differ from HVC_{RA} neurons in their I_h amplitude (two-sample $t(7) = 2.5$, $P = 0.04$ for HVC_{Av} neurons (n = 7) versus HVC_{RA} neurons (n = 7); two-sample $t(9) = 3.2$, P = 0.01 for HVC_X neurons (n = 9) versus HVC_{RA} neurons (n = 7)). HVC_{Av} neurons differ from HVC_X and HVC_{RA} neurons in **i)** the coefficient of variation of their DC-evoked interspike intervals (two-sample t(5) = 2.9, P = 0.03 for HVC_{Av} neurons (n = 7) and HVC_{RA} neurons (n = 6); two-sample t(12) = 3.0, P = 0.01 for HVC_{Av} neurons (n = 7) and HVC_X neurons (n = 9)). Scale bar, 100μm in B (left panel) and 15μm in B (right panel). Scale bar, 100μm in B and 15μm in C.

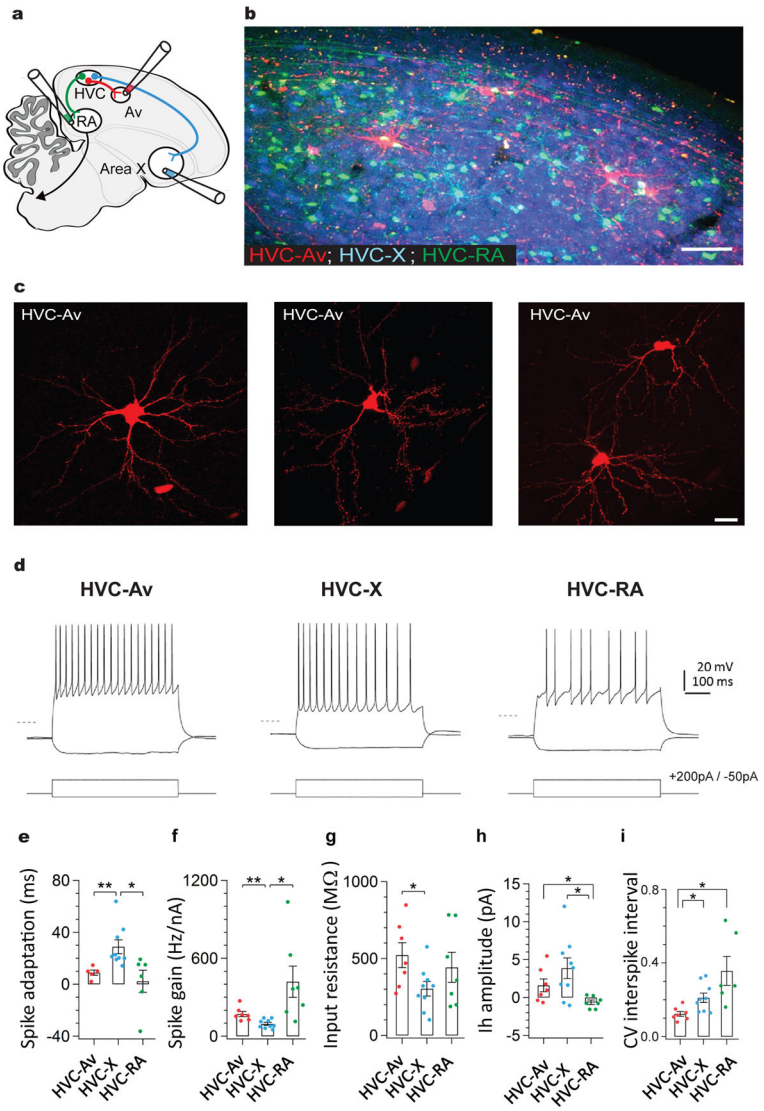

Figure 2. HVC_{Av} neurons transmit motor-related signals during song production

a) Schematic of imaging experiments employing a miniature epifluorescence microscope (Inscopix) for *in vivo* calcium imaging of HVC_{Av} neurons expressing GCaMP6s. **b)** Bulk fluorescent signal measured in HVC at rest (top left) and during singing (top right). Bottom panel shows bulk change in fluorescent signal during singing of multiple song bouts (song onset to song offset for each bout indicated by blue shading). Scale bars, 100 μm x 100 μm (top panels) and 1% and 2s (bottom panel). **c)** Average change in bulk fluorescence signals measured during singing in birds expressing GCaMP6s in HVC_{Av} neurons with their hearing intact (top panel, n=4) and after deafening (middle panel, n=2), and in a bird not injected with GCaMP (bottom panel, n=1). Onset and offset of song bout indicated by blue shading. Scale bars, 2% and 1s. **d)** Example field of GCaMP-labelled HVC_{Av} neurons imaged through miniature microscope in a singing zebra finch. Putative individual cells, which were identified with CNMF analysis, are indicated by colored outlines. Scale bars, 100 μm x 100 μm. **e)** Activity of five putative HVC_{Av} neurons indicated in panel d) during a single song

bout comprising two motifs (sound spectrogram at top; color in the sound spectrogram indicates relative power with black indicating the lowest power (during silent intervals) and red indicating the highest relative power within the vocal range). **f)** Singing related activity of five different putative HVC_{Av} neurons from the same bird from which d) and e) were collected but several days after deafening; activity is aligned to a single bout comprising two motifs. Scale bars in e) and f), 20 arbitrary activity units and 500 ms.

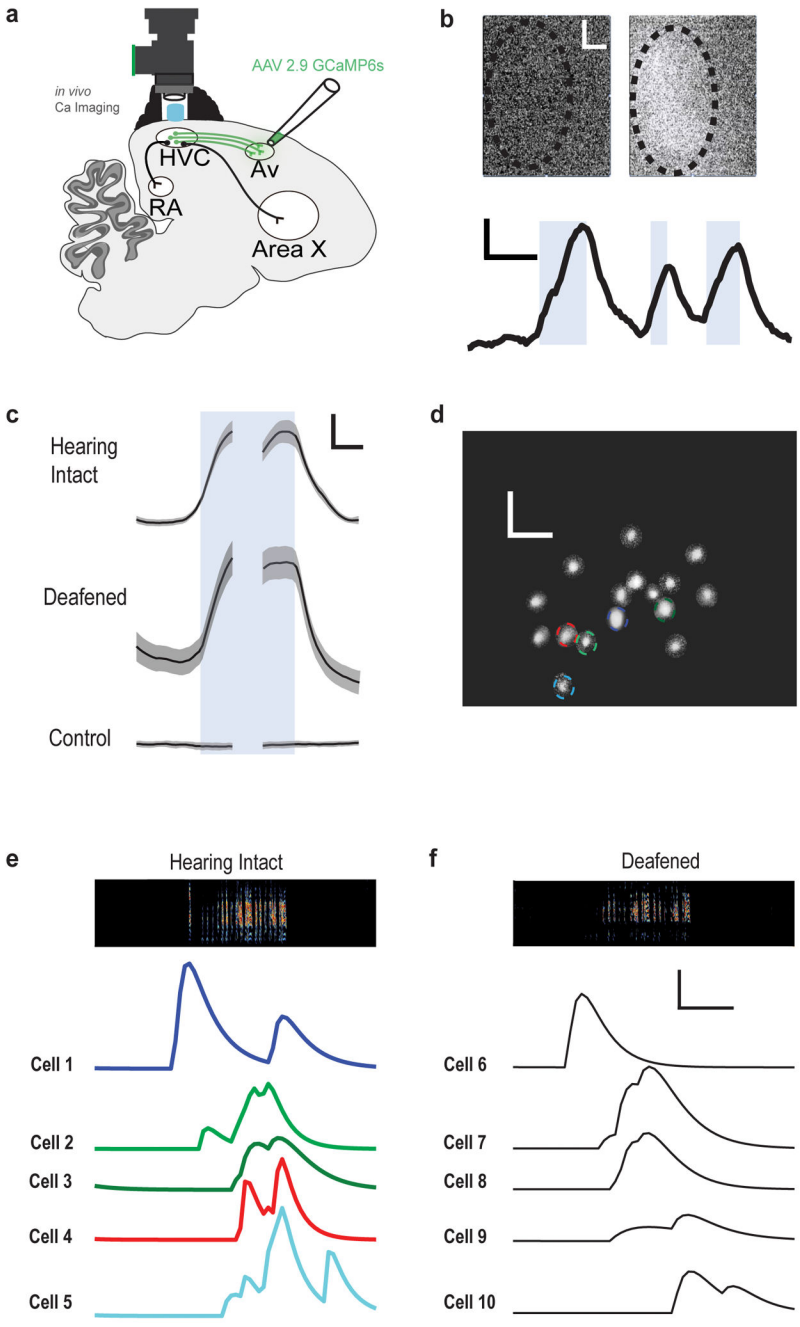

Figure 3. HVC_{Av} neurons receive selective input from premotor HVC_{RA} neurons

a) Schematic of *in vitro* brain slice preparation in which whole cell voltage clamp recordings were made from retrogradely-labeled HVC_{Av} neurons while either HVC_{RA} or HVC_X axons were electrically stimulated to evoke antidromic propagation of activity into the HVC local circuit (HVC_{RA}: 40 – 80 μA; HVC_X axons: 40 – 300 μA). Left inset, excitatory synaptic currents evoked in an HVC_{Av} neuron in response to HVC_{RA} axon bundle stimulation (80 μA). Right inset, absence of synaptic currents recorded in the same HVC_{Av} neuron following HVC_X axon bundle stimulation (160 μA; V_h = − 70 mV in both examples). **b)** Schematic of

whole cell voltage and current clamp recordings made from retrogradely labeled HVC_{RA} or HVC_X cells while electrically stimulating HVC_X axon bundles. Left inset, excitatory synaptic currents evoked in an HVC_{RA} cell following HVC_X axon bundle stimulation (80 μA; V_h = −70 mV). Right inset, antidromic action potential evoked in an HVC_X cell following HVC_X axon bundle stimulation (80 μA; V_{rest} = −80 mV). In all inset panels, individual currents or potentials are shown in gray and mean current or potential is shown in black.

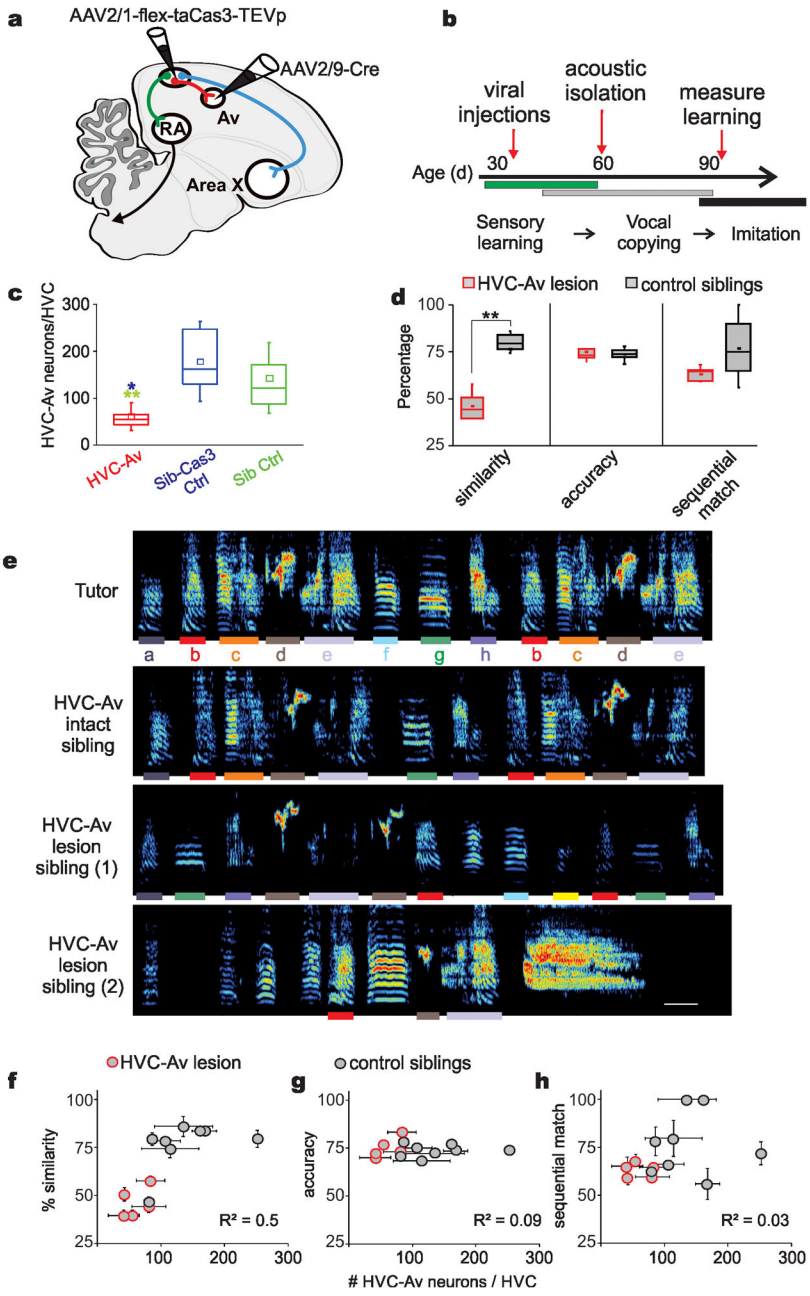

Figure 4. Intersectional genetic ablation of HVC_{Av} neurons in juvenile zebra finches impairs their ability to copy a tutor song

a) Schematic showing viral strategy for genetically ablating HVC_{Av} neurons with a Cre-dependent form of caspase 3 (Cas3). **b)** Timeline of experiments. Viral injections of AAV2/1-FLEX-taCas3-TEVp into HVC and AAV2/9-Cre-GFP into Av are made in juvenile male zebra finches between 35–40 days posthatch (dph). Birds are separated from their parents and other siblings starting at 60 dph and the quality of song copying is measured at >90 dph, when song copying is complete. **c)** The number of retrogradely labeled HVC_{Av} neurons (HVC_{Av} neurons per hemisphere) in adult birds that were injected as juveniles with both AAV2/1-FLEX-taCasp3-TEVp into HVC and AAV2/9-Cre-GFP into Av (red, HVC_{Av})

is significantly lower than the number of HVC_{Av} neurons in found in adult siblings injected as juveniles only with AAV2/1-FLEX-taCas3-TEVp into HVC (blue, Sib-Cas3 Ctrl) or adult siblings that were not injected with any virus (green, Sib Ctrl) (Mann-Whitney U(9) = 86, Z = −3.31, $P = 0.0009$ for HVC_{Av} lesioned (red) versus Sib-Cas3 (blue); Mann-Whitney U(16) = 16, Z = 3.44, $P = .0006$ for HVC_{Av} lesioned (red) versus Sib Ctrl (green)). **d)** Adult birds injected with both Cas3 and Cre at ~ 35–40 dph sang poorer copies of their tutors' songs compared to their control siblings (combined group of Sib-Cas3 and Sib Ctrl birds), as measured by song similarity% scores (see Methods) but show no difference to control siblings in measures of percent accuracy and sequential match percentage (see Methods). Tukey boxplots (**c** and **d**) show the first and third quartile of the data; the median, mean and 1.5 interquartile range are shown by the band, the dot and whiskers respectively. **e)** Example sound spectrograms from the tutor (top), from one adult pupil (control) with a normal complement of HVC_{Av} neurons, and from two adult siblings (siblings 1 and 2) in which HVC_{Av} neurons were genetically ablated during juvenile life. Color in the sound spectrogram indicates relative power with black indicating the lowest power (during silent intervals) and red indicating the highest relative power within the vocal range. Individual syllables in the tutor's song and the copied versions, defined by >70% accuracy scores, of these syllables in the pupil's adult songs are color coded by lines under each of the tutor's syllables. The control sibling's song is 78.5% similar to the tutor and this bird had 106.5 HVC_{Av} neurons per hemisphere (neurons averaged from the two hemispheres). Sibling 1's song is 50.6% similar to the tutor and this bird had 42.5 HVC_{Av} neurons, and sibling 2's song is 39.5% similar to tutor and this bird had 41.5 HVC_{Av} neurons. Scale bars: 100 msec, ordinate spans 0 – 10 kHz. Colored bars correspond to individual syllables copied from the tutor's song. **f)** Similarity of the adult bird's copy to its tutor's song plotted as a function of the average surviving numbers of HVC_{Av} neurons counted in the two hemispheres in each bird ($R^2 = 0.5$, $P = 0.004$, n = 13 birds, data are mean ± s.e.m.). **g)** Accuracy of the adult song copy as a function of average number of HVC_{Av} neurons counted in the two hemispheres from each bird ($R^2 = -0.09$, $P = 0.9$, n = 13 birds, data are mean ± s.e.m.). **h)** Sequential match of the adult copy to its tutor song as a function of average surviving number of HVC_{Av} neurons counted from the two hemispheres in each bird ($R^2 = 0.03$, $P = 0.25$, n = 13 birds, data are mean ± s.e.m.).

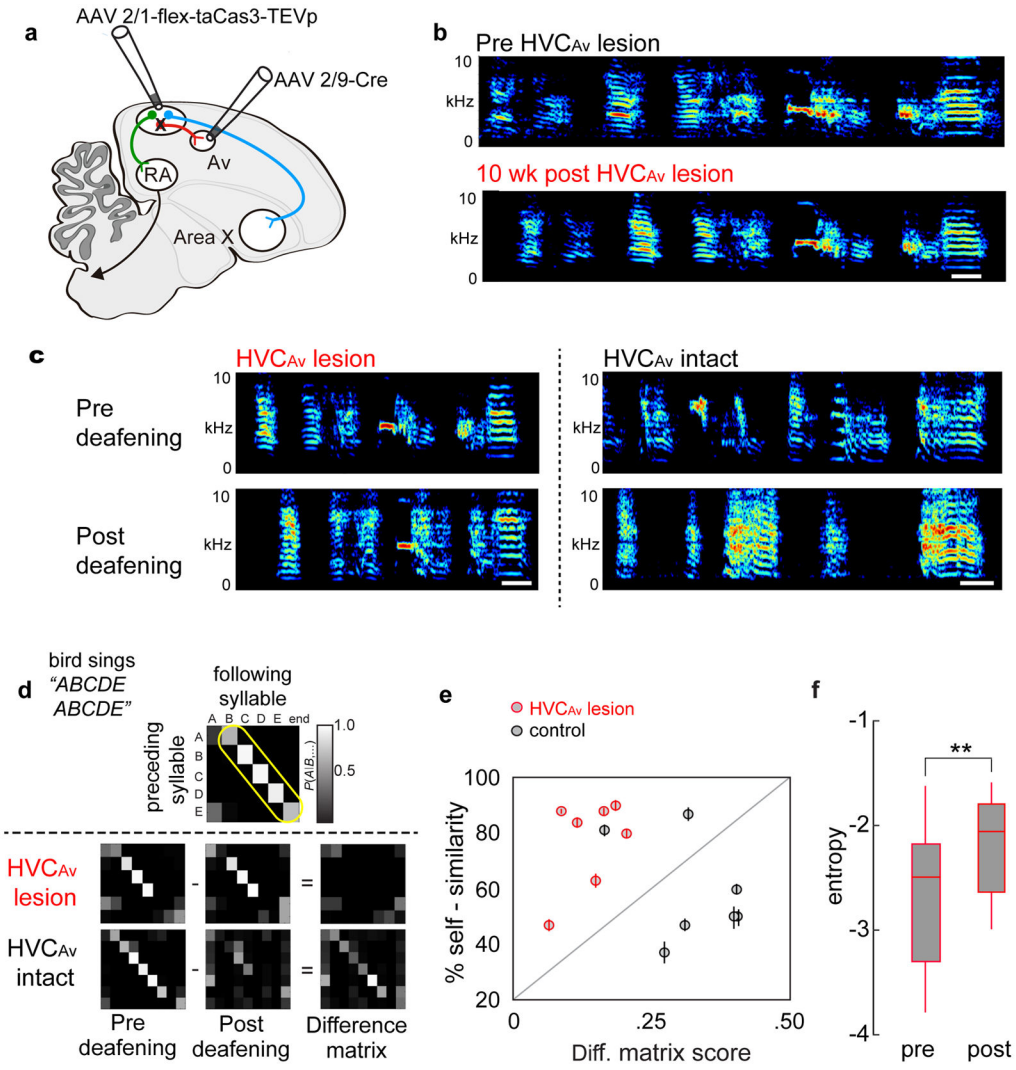

Figure 5. Intersectional ablation of HVC_{Av} neurons in adult birds does not disrupt song production but does attenuate deafening-induced degradation of song's temporal features

a) Schematic showing viral strategy for genetically ablating HVC_{Av} neurons with a Cre-dependent caspase 3 in adult birds. **b)** Sonograms recorded from an adult zebra finch before and 10 weeks after bilateral ablation of HVC_{Av} neurons reveal no evidence of song degradation (two-sample $t22 = -1.4$, $P = 0.16$ for comparisons in song self-similarity from HVC_{Av} lesioned birds (n = 12) versus control adult birds (n = 12 birds)). Color in the sound spectrogram indicates relative power with black indicating the lowest power (during silent intervals) and red indicating the highest relative power within the vocal range. **c)** Example sonograms recorded before and 10 weeks after deafening in adult zebra finches in which HVC_{Av} neurons had been previously ablated (*left*) or were intact (*right*). **d)** Song transition matrix scores, which serve as a primary measure of the linearity and stability of syllable sequences, are calculated by summing probability scores along the boxed region (*yellow* indicates core syllable transition sequence before deafening) within the matrix. Subtracting the song matrix at 10 weeks post deafening from the pre-deafening song matrix reveals little change in syllable sequence linearity and stability in birds with bilateral HVC_{Av} lesions,

whereas the difference matrix from deafened controls showed marked changes. **e)** Ablating HVC_{Av} neurons reduces the magnitude of changes to syllable sequences but not syllable features following hearing loss, as revealed by group data plotting difference matrix scores and self-similarity scores for syllables pre- and 10 weeks following deafening (n = 7 HVC_{Av} - lesioned birds, n = 7 HVC_{Av} intact birds; two-sample $t(12) = -4.8$, $P = 0.0004$ comparing difference matrix scores from lesioned versus intact birds; two-sample $t(12) = 1.9$, $P = 0.07$ comparing self-similarity scores from lesioned versus intact birds). **f)** Within-syllable comparisons reveal a significant increase in entropy before and 10 weeks after deafening in HVC_{Av} - lesioned birds (two-sample $t(11) = -4.0$, P = 0.0019).

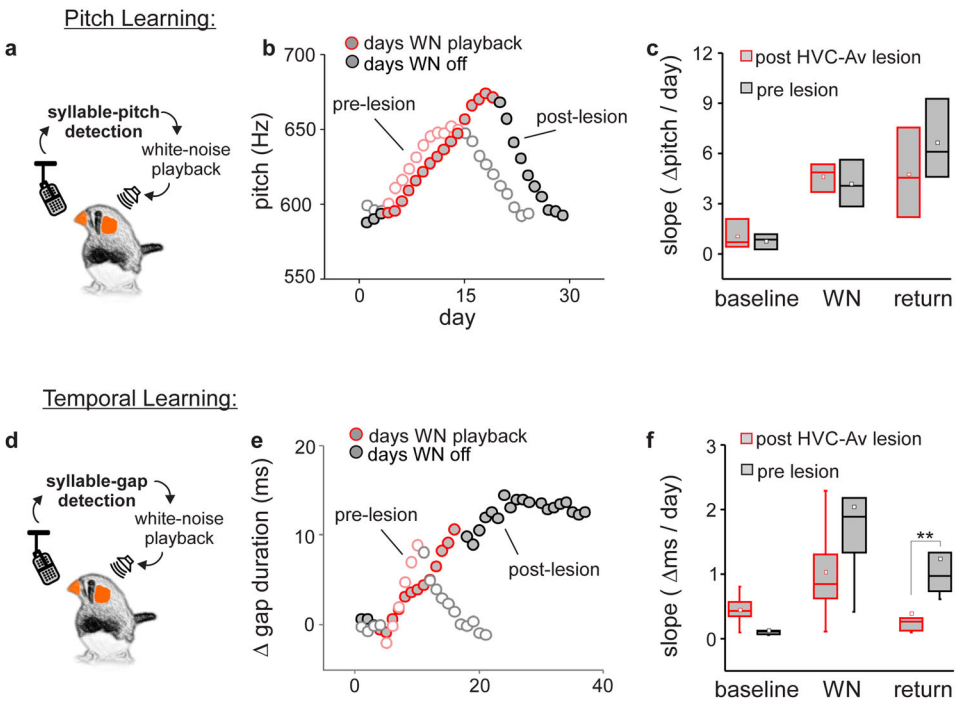

Figure 6. Intersectional ablation of HVC_{Av} neurons in adult zebra finches interferes with feedback-dependent plasticity of song element timing but not syllable pitch

a) Schematic of pitch learning paradigm. **b)** Syllable pitch (i.e., fundamental frequency) measured during pitch-contingent playback of white noise (WN; *red*) and subsequent recovery of original pitch after noise was discontinued measured in an adult male zebra finch before (unfilled circles) and after (grey filled circles) genetic ablation of HVC_{Av} neurons (average standard deviation of pitch during baseline, WN and recovery days was 9.2Hz, 9.2Hz and 10.6Hz pre-lesions and 13.0Hz, 10.9Hz and 11.3Hz post-lesion). **c)** Change in syllable pitch per day (Hz/day) before, during, and after WN playback across birds before (black) and after (red) genetic ablation of HVC_{Av} neurons. **d)** Schematic of song element duration learning paradigm. **e)** Change in song element timing in response to song element duration-contingent WN playback (*red*) and subsequent recovery of timing measured in an adult male zebra finch before (unfilled circles) and after (grey filled circles) genetic ablation of HVC_{Av} neurons (average standard deviation of song element duration during baseline, WN and recovery days was 3.9ms, 4.1ms and 3.7ms pre-lesions and 3.3ms, 3.8ms and 5.2ms post-lesion). **f)** Change in song element duration per day (ms/day) before, during, and after WN playback across birds before (black) and after (red) genetic ablation of HVC_{Av} neurons reveals a significant disruption in recovery of song timing (n = 5 birds, paired t-test $t(4) = 4.8$, $P = 0.008$). Tukey boxplots (**c** and **f**) show the first and third quartile of the data, the median, mean and 1.5 interquartile range are shown by the band, the dot and whiskers respectively.